Reduced Pyrochlores

New Oxidation States and Defect Chemistry in the Pyrochlore Structure**

*Giles D. Blundred, Craig A. Bridges, and Matthew J. Rosseinsky**

The introduction of anion vacancies into complex metal oxides is a powerful method of controlling structure and properties by tailoring metal coordination environment and oxidation state. The hydride anion can effect reductive transformations of oxides inaccessible to conventional metal getters or gaseous reducing agents.[1] The $A_2B_2O_7$ pyrochlore structure[2] is important for properties as diverse as anion and mixed conduction,[3] superconductivity,[4] and colossal magnetoresistance,[5] but, in contrast to ABO_3 perovskite, there is little chemistry established for the low-temperature introduction of anion vacancies and generation of associated defect structures. Pyrochlore is well known for stabilizing high oxidation states on the octahedral B site; A^{II}/B^{V} and A^{III}/B^{IV} compositions are well established, and pyrochlores with mean B site oxidation states of less than +4 are rare (the Y^{II}/Ti^{II} pyrochlore-related $YTiO_{2.1}$ prepared at 2800 °C is the sole example[6]). Here we report the systematic low-temperature synthesis of pyrochlore systems with up to 90% titanium(III) on the octahedral sites.

[*] Dr. G. D. Blundred, Dr. C. A. Bridges, Prof. Dr. M. J. Rosseinsky
Department of Chemistry
The University of Liverpool
Liverpool L69 7ZD (UK)
Fax: (+44) 151-794-3587
E-mail: m.j.rosseinsky@liv.ac.uk

[**] We thank the UK EPSRC and the ACS Petroleum Research Foundation for support.

Supporting information for this article is available on the WWW under http://www.angewandte.org or from the author.

  DOI: 10.1002/ange.200453819

The $A_2B_2O_6O'$ pyrochlore structure (Figure 1a) is a corner-sharing network of BO_6 octahedra with large 110 tunnels intersecting at the 8b positions (space group $Fd\bar{3}m$) occupied by the O′ oxygen atoms. The A cations are eight-coordinate (2 O′ and 6 O anions). The structure can also be described as an anion-deficient, vacancy-ordered fluorite, in which the 8a anion sites at the centroids of tetrahedra of 16c B sites are vacant. This defect ordering renders the B sites octahedral, while the tetrahedral connectivity of both A and B sublattices gives rise to strong geometrical frustration[7] of antiferromagnetic ordering, manifested in the unusual magnetism of the rare earth A^{3+} sublattice in $Ln_2Ti_2O_7$[8] and of the B site cations in materials such as $NH_4Fe_2F_6$[9,10] and $Y_2Mn_2O_7$.[11] This makes the introduction of localized 3d $S = {}^1/_2$ spins on the B sublattice an important synthetic task.

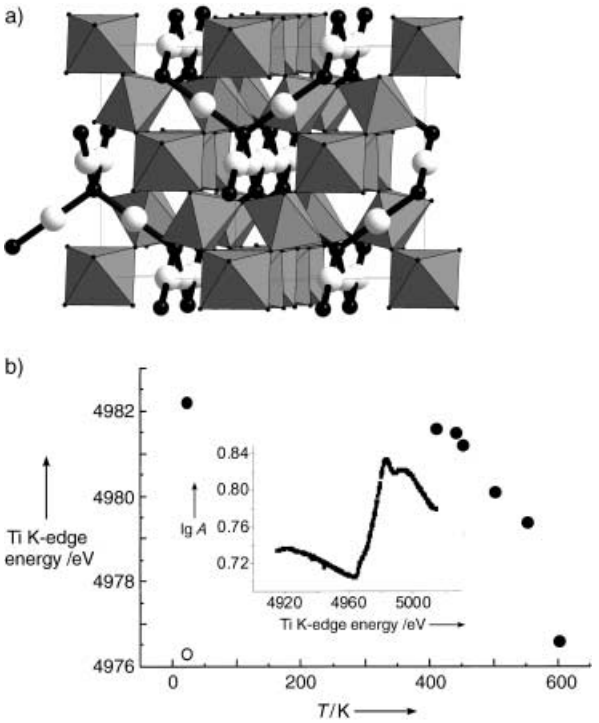

Figure 1. a) The BO_6 (gray octahedra) and A_2O' sublattices (A white spheres, O′ black spheres), showing the two independent oxygen networks in the pyrochlore structure. b) Position of the Ti X-ray absorption K-edge (black circles) in $Lu_2Ti_2O_{7-y}$ as a function of reaction temperature with CaH_2. The open circle marks the edge position in $LuTiO_3$. The inset shows data for the sample reduced at 600 °C ($y = 0.9$).

The Ti^{IV} pyrochlores $Ln_2Ti_2O_7$ are not reduced by hydrogen gas at 1200 °C. Reaction with metal hydride (LiH, CaH_2) reducing agents below 700 °C, however, affords intensely black material which retains the pyrochlore structure: the absence of $h = 4n$, $k = 4n$, $l = 2n$ reflections shows that the cations remain on the 16c and 16d sites.[12]

The reactivity of $Ln_2Ti_2O_7$ with CaH_2 is sensitively controlled by the size of the Ln^{III} cation. $Sm_2Ti_2O_7$ and $Eu_2Ti_2O_7$ form the titanium(III) perovskites $SmTiO_3$ and $EuTiO_3$ at 600 °C, but smaller lanthanides afford reduced pyrochlores. The lowest Ti oxidation states are accessible with Lu and Yb. X-ray absorption spectroscopy demonstrates reduction at the Ti rather than the lanthanide site in both $Yb_2Ti_2O_7$ and $Lu_2Ti_2O_7$, as the lanthanide L_{III} edge positions remain unchanged in the reduced materials. The extent of reduction varies with reaction temperature, and reaction at above 600 °C affords the 90 % titanium(III) phase $Lu_2Ti_2O_{6.10}$. It remains to be established whether single-phase materials with continuously varying oxygen content over the entire oxidation state range between titanium(III) and titanium(IV) can be prepared. Figure 1b shows the evolution of the Ti K-edge from 4982.2 eV in the titanium(IV) starting material to 4976.6 eV in $Lu_2Ti_2O_{6.10}$ reduced at 600 °C, comparable to the edge position in the titanium(III) phase $LuTiO_3$. Transmission electron micrographs revealed that crystallinity is retained during reaction without the formation of amorphous material, and EDX analysis demonstrated that Ca is not included into the pyrochlore crystallites during the reaction.

Reaction of $Yb_2Ti_2O_7$ with one equivalent of CaH_2 at 600 °C followed by washing with 0.1 M NH_4Cl in methanol under nitrogen to remove CaO affords $Yb_2Ti_2O_{6.45}$, which is single-phase to synchrotron X-ray powder diffraction (Figure 2b). Refinement of neutron powder diffraction data from

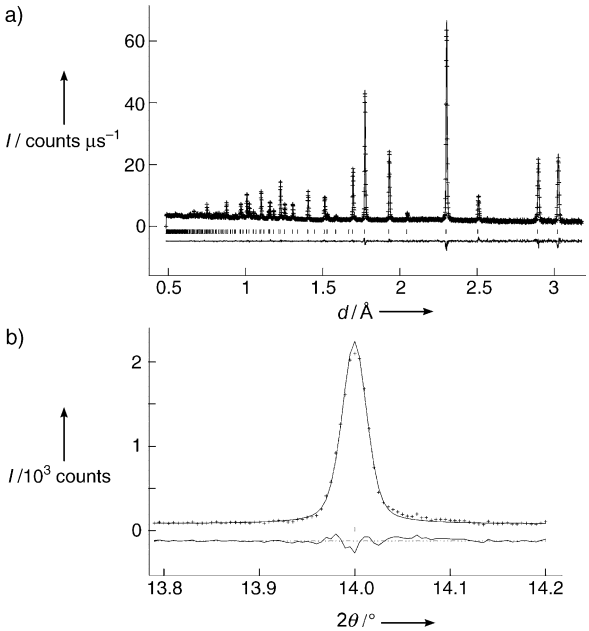

Figure 2. a) Rietveld refinement of powder neutron diffraction data from $Yb_2Ti_2O_{6.43}$ (POLARIS diffractometer, ISIS. $\chi^2 = 1.18$, $R_{wp} = 2.21$ %; $R(F^2) = 6.50$, $R(F) = 4.04$ %). b) Rietveld fit to the 222 reflection from $Yb_2Ti_2O_{6.43}$ (station 9.1, Daresbury SRS, $\chi^2 = 1.10$)

$Yb_2Ti_2O_{6.45}$ (Figure 2a) revealed preferential loss of anions from the O (83 % occupancy) rather than the O′ network and the presence of 3.3 % antisite disorder of Yb and Ti that was not present in the starting material. Electron diffraction showed that the anion vacancies remain disordered over shorter length scales than those probed by X-ray and neutron diffraction. The 8a anion site, vacant in the parent structure, is partially occupied. The extent of antisite disorder and associated structural relaxation is more pronounced in the

$Lu_2Ti_2O_{6+x}$ phases prepared under the same conditions, and so the structure of these materials was considered in more detail.

$Lu_2Ti_2O_{6.43(1)}$ (Table 1; see Supporting Information) has 6.7(6) % antisite disorder between the two cation sublattices, 85(1) % O48f (O2 in Table 1) and 91(2) % O′ (O1) occupancy of the original oxygen positions, and two new defect anion positions. Scattering density in the vicinity of the 8a sites (equivalent to 20 % of an oxide anion) corresponds to occupancy of the 32e O3 site tetrahedrally disposed around the 8a center. The 8a site is vacant in the parent pyrochlore structure and coordinates only to the octahedral B sublattice array. The second defect O4 is 0.8 Å from the bulk 48f O2 site.

Table 1: Refined coordinates for $Lu_2Ti_2O_{6.43(1)}$.[a]

	x	y	z	U_{equiv} [Å^{-2}]	Site occupancy
Ti1/Lu2[b] 16c	0.000000	0.000000	0.000000	0.0089	0.934(6)
Lu1/Ti2[b] 16d	0.500000	0.500000	0.500000	0.023	0.934(6)
O1 8b	0.375000	0.375000	0.375000	0.014	0.912(17)
O2 48f	0.3370(2)	0.125000	0.125000	0.028	0.849(12)
O3 32e	−0.396(3)	0.1464(30)	−0.3964(30)	0.05(1)	0.045(4)
O4 48f	−0.424(6)	−0.125000	−0.125000	0.05(1)	0.041(4)

[a] $a = 10.01728(21)$ Å, space group $Fd\bar{3}m$. [b] Site occupancies were refined such that the antisite (Lu2, Ti2) and (Lu1, Ti1) main sublattice occupancies at each site summed to 1.00. The number quoted is the main sublattice occupancy. Anisotropic displacement parameters for the bulk sites are listed in the Supporting Information

The O3 oxygen defect is coordinated to Ti and locally controls occupancy of the O2 48f site. The O3 site is displaced from the 8a site towards the center of one of the triangular faces of the B_4 tetrahedron of neighboring Ti sites, creating one long and three shorter Ti–O3 contacts (Figure 3a).

The shorter Ti–O3 distance of 2.075 Å corresponds to the defect anion being located 1.94 Å from two of the bulk O2 48f sites, and this requires that in the vicinity of the 8a defect these two sites must be vacant (Figure 3b). This means that these 15 % of the Ti sites have only four O2 neighbors that produce a five-coordinate distorted trigonal-bipyramidal environment around the Ti center with a valence sum of +2.92, consistent with occupancy of this site by Ti^{III}. The mean coordination number of 5.1 of the octahedral B site by O2, determined by its refined occupancy, is then assigned as 15 % of Ti sites fourfold-coordinated by O2 in the above-mentioned trigonal bipyramids involving the O3 defect, 25 % six-coordinate (valence sum +3.9), and 60 % five-coordinate (valence sum +3.3), that is, three distinct Ti environments with a mean valence sum of +3.39 close to that expected from the TGA-derived composition.

The displacement of O3 from the center of the 8a site occurs to shorten the Ti–O distance to less than 2.168 Å. The Lu2 cations occupying the Ti sublattice due to the antisite disorder correspond to the longer (2.54(5) Å) Ti–O3 contacts. The distorted cubic environment (Figure 3c) is completed by six Lu2–O4 contacts of 2.48(5) Å to the O48f-related O4 defect anion. The calculated valence sum of +2.3 indicates underbonding and further local relaxation of the anions associated with this site. The Ti2 cations occupying the Lu sublattice correspond to absent O′ anions and are octahedrally coordinated by six O4 anions at 1.93(3) Å, with a valence sum of +4.4. The imperfect quantitative description of the bonding at both antisite cation defects can be associated with the use of only one position to describe the defect anion sites.

Removal of oxygen from $A_2B_2O_6O'$ pyrochlore poses the question of whether vacancies will be formed on the structurally distinct O or O′ sublattices. Anion-deficient pyrochlores containing lone-pair cations such as Pb^{II} lose anions from the O′ site (e.g., $Pb_2Ru_2O_{6.5}$),[13] whereas isovalent B site disorder in $Ln_2Ti_{2-x}Zr_xO_7$ favors anion transfer from the O 48f to the 8a sites,[14] consistent with modeling.[15] In $Ln_2Ti_2O_{6+x}$ oxygen vacancies are formed on the O sublattice, as reduction occurs solely at the Ti centers which are not bound to O′. The cation antisite disorder reflects the movement of O2 in response to reduction of the B cation. This

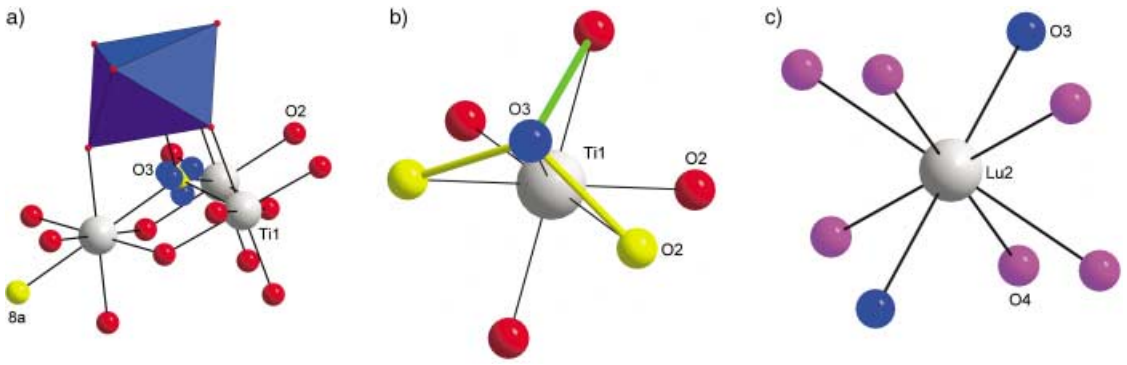

Figure 3. Anion defects and cation coordination in $Lu_2Ti_2O_{6.43}$. Distances and angles are given in the Supporting Information. a) The O3 oxygen atom on the 32e site (blue spheres) is displaced from the center of the 8a site (yellow sphere), which is vacant in the perfect parent pyrochlore structure. b) The O3 site is only occupied at Ti sites where two O2 sites (marked as yellow spheres linked by short yellow contacts of 1.94 Å; these are the 48f anion positions in the parent structure) are vacant, producing a five coordinate site. The green contact indicates the closest remaining O3–O2 distance of 2.37 Å, acceptably close to the 2.56 Å O2–O2 contacts in view of the 0.1 Å rms anion displacement ellipsoids. c) The distorted cubic arrangement of O3 (blue) and O4 anions around the Lu antisite cations on the octahedral Ti sublattice.

lengthens the B–O2 and shortens the A–O2 bonds, and this opens up the possibility of antisite disorder of the lanthanide and titanium cations, the smaller Lu^{III} giving more extensive disorder. The occupation of the O3 defect site is a disordering of the parent pyrochlore (where differentiation between the A and B sites arises from ordering of the anion vacancies onto the 8a site that is now partially occupied) towards the fluorite structure, as observed for lanthanide zirconates which adopt both ordered (pyrochlore) and disordered (fluorite) structures.[16]

A strong motivation for preparing titanium(III) pyrochlores is to study the behavior of $S = 1/2$ centers on the geometrically frustrated B site pyrochlore lattice (synthetic procedures which minimize the antisite disorder are required if materials of this class are to be genuine model systems); the 3d electrons introduced at the Ti^{III} sites are localized, as evidenced by the persistence of the Ti–O phonons in the IR transmission spectra of the reduced materials. Magnetization measurements (Figure 4) indicate that the localized spins at

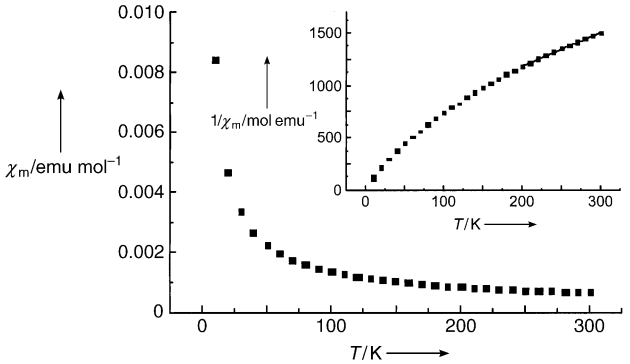

Figure 4. Magnetic susceptibility at 1.5 T and Curie–Weiss fit (inset) for $Lu_2Ti_2O_{6.10}$.

the Ti centers are strongly coupled antiferromagnetically: Curie–Weiss fits to $Lu_2Ti_2O_{6+x}$ ($x = 0.1$, 0.5) are both only valid at high temperature and give moments at the Ti sites that are lower than expected (1.12(1) μ_B per Ti ($x = 0.1$), 0.88(3) μ_B per Ti ($x = 0.5$), compared with predicted 1.64 μ_B and 1.23 μ_B) with Weiss constants of −173(6) K and −227(17) K. The moment suppression is qualitatively consistent with strong antiferromagnetic coupling between the Ti centers that is geometrically frustrated (the tetrahedral plaquette is shown in Figure 3a) against long-range order by the tetrahedral geometry of the B sublattice (no additional magnetic Bragg peaks are observed in neutron diffraction at 5 K from the Lu or Yb phases discussed above). This motivates further detailed studies of the electronic properties of this new class of defect pyrochlore by muon spin relaxation (μSR) and neutron scattering.

Received: January 21, 2004 [Z53819]

Keywords: lanthanides · magnetic properties · pyrochlore phases · reduction · titanium

[1] M. A. Hayward, E. J. Cussen, J. B. Claridge, M. Bieringer, M. J. Rosseinsky, S. J. Blundell, I. M. Marshall, F. L. Pratt, *Science* **2002**, *295*, 1882–1884.
[2] M. Subramanian, G. Aravamudan, G. C. Subba Rao, *Prog. Solid State Chem.* **1983**, *15*, 55.
[3] O. Porat, C. Heremans, H. L. Tuller, *Solid State Ionics* **1997**, *94*, 75–83.
[4] M. Hanawa, Y. Muraoka, T. Tayama, T. Sakakibara, J. Yamaura, Z. Hiroi, *Phys. Rev. Lett.* **2001**, *87*, 187001.
[5] Y. Shimakawa, Y. Kubo, T. Manako, *Nature* **1996**, *379*, 53–55.
[6] S. Mohr, H. Müller-Buschbaum, *J. Alloys Compd.* **1994**, *210*, 115–118.
[7] S. T. Bramwell, M. J. P. Gingras, *Science* **2001**, *294*, 1495–1501.
[8] A. P. Ramirez, B. S. Shastry, A. Hayashi, J. J. Krajewski, D. A. Huse, R. J. Cava, *Phys. Rev. Lett.* **2002**, *89*, 067202.
[9] G. Ferey, M. Leblanc, R. Depape, J. Pannetier, *Solid State Commun.* **1985**, *53*, 559–563.
[10] G. Ferey, R. Depape, M. Leblanc, J. Pannetier, *Rev. Chim. Miner.* **1986**, *23*, 474–484.
[11] J. N. Reimers, J. E. Greedan, R. K. Kremer, E. Gmelin, M. A. Subramanian, *Phys. Rev. B* **1991**, *43*, 3387–3394.
[12] J. L. Fourquet, H. Duroy, P. Lacorre, *J. Solid State Chem.* **1995**, *114*, 575–584.
[13] R. A. Beyerlein, H. S. Horowitz, J. M. Longo, M. Leonowicz, *J. Solid State Chem.* **1984**, *51*, 253–265.
[14] C. Heremans, B. J. Wuensch, J. K. Stalick, E. Prince, *J. Solid State Chem.* **1995**, *117*, 108–121.
[15] M. Pirzada, R. W. Grimes, L. Minervini, J. Maguire, K. E. Sickafus, *Solid State Ionics* **2001**, *140*, 201–208.
[16] J. Chen, J. Lian, L. M. Wang, R. C. Ewing, R. G. Wang, W. Pan, *Phys. Rev. Lett.* **2002**, *88*, 105901.

